On the Definition of Radar Range Resolution for Targets of Greatly Differing RCS

Hasan S. Mir, *Senior Member, IEEE*, and Blair D. Carlson, *Senior Member, IEEE*

***Abstract*—Conventional radar system design uses only waveform bandwidth to measure the range resolution. This paper examines the effect of both bandwidth and the difference in target radar cross section on range resolution. In the context of the subject scenario, the nature of the pulse-compressed return is studied, and a commonly used measurement definition of range resolution that assumes equally reflective targets is extended to account for the difference in target reflectivity as well. Results are presented as an application of the derived results to depict how resolution performance is affected by various parameters and how a more comprehensive definition of range resolution can be used during the system design.**

***Index Terms*—Radar, radar cross section (RCS), range resolution, resolution bound, unequal targets.**

I. Introduction

A KEY performance parameter of a radar is its ability to resolve two targets that are closely spaced in range. Such an ability allows for distinction between scatterers originating from separate targets or from a larger extended target.

Much work has been conducted into the design of methods and systems to obtain high-resolution target scattering profiles [1]–[13]. Amongst the earliest works in this area, [1] examined the fundamental tradeoff between localization in time and localization in frequency, arriving at the (now well-known) conclusion that the "optimal" radar waveform for generating a high-resolution profile is one that is simply matched to the environment. Thus, a waveform with wide bandwidth, e.g., coarse localization in frequency, will have high range resolution or fine localization in time. In practice, when generating high-range-resolution profiles for targets like aircraft/missiles, the target is illuminated with a wideband waveform from a variety of perspectives in order to develop a database of the variations in range profile that exist with the angle of waveform illumination. Compared to low-resolution profiles in which a target may be confined to a single range gate, high-resolution profiles provide information on the spatial distribution of target reflectivity [3], [4]. This can be useful in distinguishing closely spaced targets or in determining the features of an extended target. The latter application can be used for the purpose of target identification when matched to a database generated as previously described. However, when digital receivers are employed (as is increasingly common), the usage of wideband waveforms necessitates high-speed digital acquisition and processing systems, posing an overburdening of the digital receiver. Use of stepped-frequency waveforms in such a situation is a possible alternative. In [5], an air-to-ground radar system is described that employs a programmable waveform generator to achieve high range resolution through the use of stepped-frequency waveforms. Since this type of effectively wideband waveform is instantaneously narrowband, high-speed digital processing is eliminated since only narrowband waveforms are processed. This method is effective if the individual scattering centers on the target are relatively insensitive to frequency, thereby allowing extraction from stepped-frequency waveforms of the spatial distribution of the backscattered sources.

In addition to high-resolution measurement systems, signal processing techniques for such systems have also received much attention. In [7], a two-point scatterer model is used for bandwidth extrapolation. The Burg algorithm is then used to yield improved resolution compared to the native resolution yielded by the original radar data. References [8] and [9] discuss received-signal parameter estimation techniques using evolutionary algorithms such as particle swarm optimization. Reference [10] offers the novel idea of designing a mismatched filter. Against the conventional approach of enhancing the mainlobe frequencies, it proposes to employ a filter to enhance the sidelobe frequencies and attenuate the mainlobe frequencies. This approach increases the principal spectral bandwidth, thereby improving the range resolution. This, however, is at the cost of a substantial reduction in SNR. In [11], oversampling is applied to discrete-level waveforms. The presence of extraneous bandwidth from the level transitions is used to improve the resolution through the use of an adaptive pulse compression method. In [12], the recent technique of compressed sensing is applied to the radar problem. Through the use of waveforms with particular properties coupled with results from sparse signal representation, the need for a matched filter at the receiver is eliminated, and improved range resolution is possible due to the elimination of range sidelobes. As the authors of [12] note, however, the paradigm, as presented, has been highly abstracted, and many issues related to the practical implementation remain.

Despite the seminal contributions of such work, an underlying assumption is that range resolution is given by the

Manuscript received February 6, 2011; revised June 21, 2011; accepted July 22, 2011. This work was supported in part by a Faculty Research Grant from the American University of Sharjah FRG11-III-18 and in part by the Department of the Navy under U.S. Air Force Contract FA8721-05-C-0002. The Associate Editor coordinating the review process for this paper was Dr. Sergey Kharkovsky.

H. S. Mir is with the American University of Sharjah, Sharjah, U.A.E. (e-mail: hmir@aus.edu).

B. D. Carlson is with Lincoln Laboratory, Massachusetts Institute of Technology, Lexington, MA 02420-9108 USA.

Color versions of one or more of the figures in this paper are available online at http://ieeexplore.ieee.org.

Digital Object Identifier 10.1109/TIM.2011.2170371

expression $c/2B$, where c is the speed of light and B is the waveform bandwidth. Such an expression, however, does not account for how range resolution is affected when the strength and radar cross section (RCS) of the targets greatly differ. As noted in [14], usage of the term RCS may be misleading due to effects such as shadowing. This term, however, is used in this paper in view of the fact that it does provide a measure of target reflectivity.

In [15], the effect of differences in target RCS is studied, and it is argued that a proper definition of range resolution should not only check for two distinct peaks in the received signal but should also account for the deviation in the apparent location of these peaks from their actual location (a quantitative measurement definition of resolution, however, is left as an open problem). In the author's previous paper [16], [17], the effect of differences in target RCS was studied using a similar resolution metric motivated by prior work on the resolution of direction of arrival estimation [18], [19].

The objective of this paper is to develop a measurement definition of range resolution (as opposed to the design of a high-resolution system [1]–[6] or resolution algorithm [7]–[12]) which relates not only waveform bandwidth but also the difference in the RCS of the two targets. Additionally, a measurement definition is sought to include another important effect (as noted in [15]) of deviation of the apparent target location from its true location.

It may be noted that [16] approaches the resolution problem from a probabilistic point of view. As such, the resulting expressions are such that for a given SNR, the difference in RCS of the targets, and target separation, the *probability* of resolving the two targets can be determined. In this paper, a measurement definition is developed so that for a given bandwidth, difference in RCS, and tolerable difference between actual and apparent target locations, the *actual range resolution* (rather than the probability of resolution) can be determined. From a practical perspective, a deterministic expression allows for quick insight into the expected baseline system performance in high-SNR environments. *The results are used to develop a basic understanding of how various parameters affect resolution performance, and thus provide a guideline for a more comprehensive definition of range resolution that can be used when designing a radar system*.

This paper is organized as follows. Section II formulates the problem and develops a new measurement definition for range resolution that accounts for the difference in target strength. Section III presents computational and experimental examples of the results developed in Section II.

II. Development

Consider two point scatterers with respective strength (RCS) and range locations of σ_k and R_k, $k = 1, 2$. It will be assumed in this paper that the pulse-compressed return from a single point target follows a Gaussian profile, and may thus be described as

$$f_k(r) = \sigma_k e^{-\beta(r-R_k)^2} \tag{1}$$

where r is the range variable and β is related to the radar waveform bandwidth B through the expression

$$B = \frac{c}{4}\sqrt{\frac{\beta}{\ln 2}} \tag{2}$$

where (2) is derived by assuming that the half-power bandwidth of (1) is equal to $c/2B$.

The assumption of the Gaussian profile is selected for several reasons. The choice of a Gaussian model often simplifies the analysis of many problems. While a parabolic shape could have been selected, it is observed that a parabola is simply the second-order approximation of the Gaussian profile. Additionally, the Gaussian profile not only obeys the requisite properties of an ambiguity function (even and nonnegative with maximum at target location) but also matches any such function or likely filter shape up to fourth order.

The pulse-compressed return for two point targets is developed as follows. The return signal after matched filtering can be expressed as

$$\mathfrak{P}(r) = \sum_{k=1}^{2} p_0(r) e^{+j\phi_k} \tag{3}$$

where $p_k(r) = \sqrt{f_k(r)}$ and ϕ_k is a phase offset. Taking the magnitude squared of (3) yields the pulse-compressed return

$$\begin{aligned}\mathfrak{F}(r) &= \|\mathfrak{P}(r)\|^2 \\ &= \sum_{k=1}^{2} p_k^2(r) + 2\cos(\phi) p_1(r) p_2(r).\end{aligned} \tag{4}$$

In (4), the value of $\phi = \phi_2 - \phi_1$ is affected by a number of parameters, such as center frequency, target separation, and various radar system effects. In order to assess the average behavior of the matched-filter output, it is assumed that ϕ is a random variable uniformly distributed on $[-\pi, +\pi]$. Thus, taking the statistical expectation of (4) yields

$$\begin{aligned}F(r) &= E\{\mathfrak{F}(r)\} \\ &= \sum_{k=1}^{2} f_k(r).\end{aligned} \tag{5}$$

Fig.1(a)–(e) shows various resolution scenarios. In Fig. 1(a), two equal amplitude scatterers are located at a range of R_1 and R_2. When the peaks of the target in the pulse-compressed spectrum are clearly separated as in Fig. 1(a), it is a simple matter to resolve the targets. However, as targets become closer in range, the peaks begin to merge, and a loss of resolution quality occurs. In order to develop a quantitative definition of this loss, it is observed from Fig. 1(a) that resolution constitutes two mathematical properties, namely, the existence of a peak around R_1 and R_2, and, as a consequence, the existence of a dip (i.e., local minimum) at

$$R_m = \frac{1}{2}(R_1 + R_2) \tag{6}$$

the halfway point between R_1 and R_2. Moreover, the quality of the resolution can be gauged by the amount that the amplitude

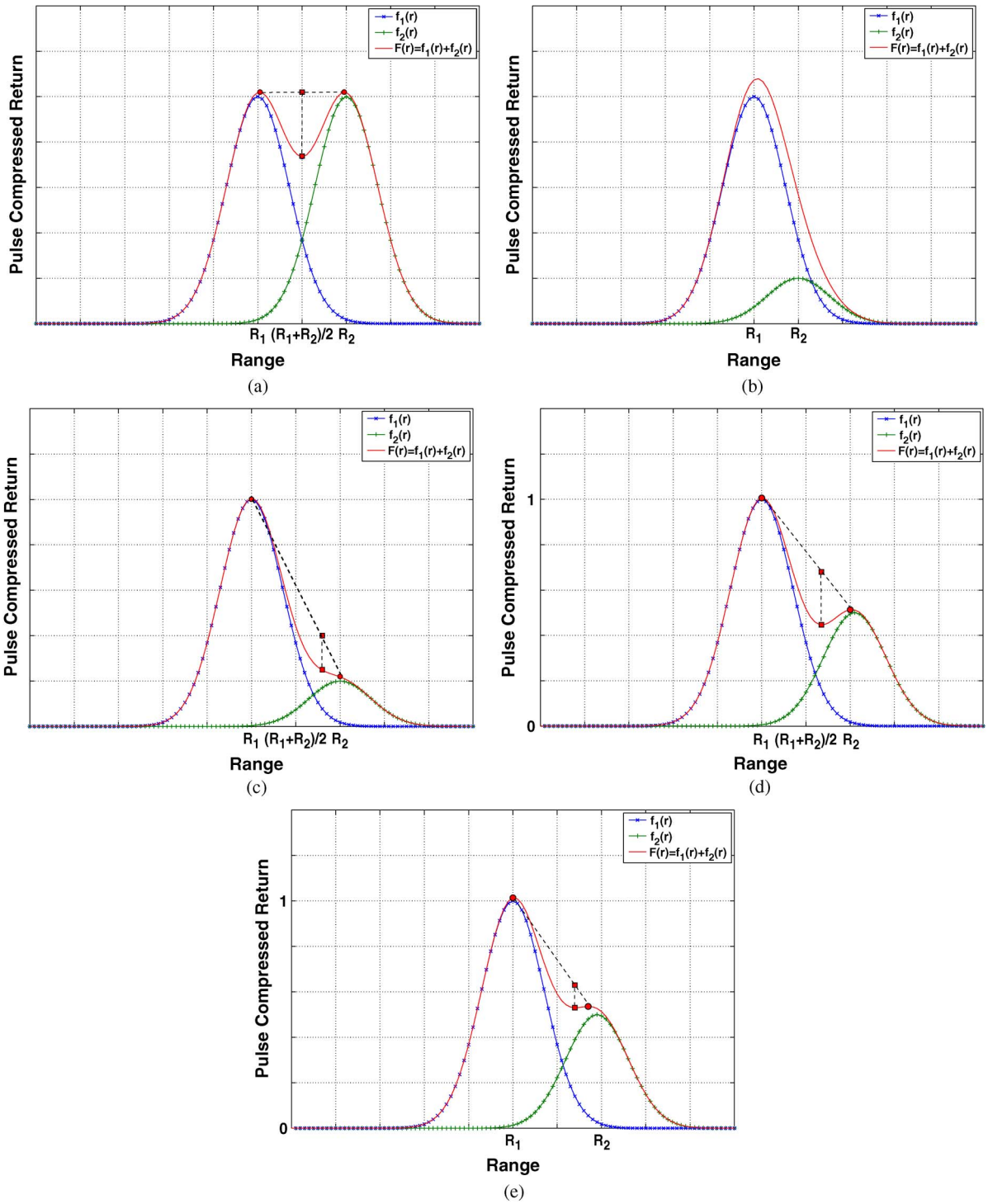

Fig. 1. (a) Pulse-compressed return of two resolved equal amplitude targets. (b) Pulse-compressed return of two unresolved unequal amplitude targets—Case 1. (c) Pulse-compressed return of two unresolved unequal amplitude targets—Case 2. (d) Pulse-compressed return of two resolved unequal amplitude targets (clearly resolved). (e) Pulse-compressed return of two resolved unequal amplitude targets (poorly resolved).

of the peaks is above the amplitude of the local minimum. Thus, resolution can be defined as the event that a local minimum exists around R_m *and* $\varepsilon > 0$, where ε is expressed as

$$\varepsilon = \frac{1}{2}\left(F(R_1) + F(R_2)\right) - F(R_m). \tag{7}$$

The metric (7) suggests that two targets are resolved so long as there exists a dip at the midpoint of the parameters of the two targets. The term $(1/2)(F(R_1) + F(R_2))$ simply averages out any small variation in the height of the spectral peaks, since $F(R_1) \approx F(R_2)$ for targets with identical (or similar) RCS. This metric has been employed in previous quantitative studies of resolution (i.e., [16]–[18]).

Fig. 1(b) and (c) shows situations which, in this paper, will be deemed as unresolvable. While lack of resolution is obvious in Fig. 1(b), it is not so obvious in Fig. 1(c). It is observed

that while such a scenario satisfies the criterion $\varepsilon > 0$, no local minimum exists between R_1 and R_2. Hence, the targets will be treated as unresolvable.

Fig. 1(d) shows the pulse-compressed return for two targets that are of differing strength. While it is expected that the amplitude of the peaks around R_1 and R_2 will thus differ, it is important to note additional effects: The location of the spectral peaks deviates slightly from R_1 and R_2, and the "dip" deviates from R_m. As such, the definition of ε in (7) should be appropriately modified.

Towards this end, the critical points of the pulse-compressed return are characterized. Denoting the actual locations of the spectral peaks and local minimum as $\hat{R}_1$, $\hat{R}_2$, and $\hat{R}_m$, respectively, a straightforward extension of (7) is to replace R_1, R_2, and R_m with $\hat{R}_1$, $\hat{R}_2$, and $\hat{R}_m$, respectively. However, such a modification is simply comparing the average height of the spectral peaks to that of the local minimum. This is relatively insensitive to the difference between the amplitude of the local minimum and the amplitude of the weaker target. For example, it is clear that the targets in Fig. 1(d) are better resolved than that in Fig. 1(e). However, applying (7) to Fig. 1(d) yields a value of $\varepsilon = 0.3$, while applying (7) to Fig. 1(e) yields a value of $\varepsilon = 0.27$, which leads to the misimpression that the resolution quality is similar.

By examining Fig. 1(d) and (e), the geometrical concept behind the intuitive notion of resolution (and, hence, the definition of ε) becomes clear: The line joining the peak at $F(\hat{R}_1)$ and $F(\hat{R}_2)$ must be above $F(\hat{R}_m)$. This can be mathematically expressed as $\hat{\varepsilon} > 0$, where

$$\hat{\varepsilon} = \frac{F(\hat{R}_2) - F(\hat{R}_1)}{\hat{R}_2 - \hat{R}_1}(\hat{R}_m - \hat{R}_1) + F(\hat{R}_1) - F(\hat{R}_m). \quad (8)$$

By way of comparison, applying (8) to Fig. 1(d) and (e) yields the values of $\varepsilon = 0.26$ and $\varepsilon = 0.1$, respectively. Hence, the difference in the value of ε as such is definitively representative of the resolution quality. Note that (8) is the natural extension of (7) to unequal amplitude targets; indeed, when $F(R_1) = F(R_2)$, (8) and (7) become the same expression.

Although analytical expressions for $\hat{R}_1$, $\hat{R}_2$, and $\hat{R}_m$ cannot be obtained, it is observed that because the behavior of $F(r)$ about the critical points is nearly parabolic, the slope of $F(r)$ about these points changes in an approximately linear manner. Thus, $dF(r)/dr$ can be expanded as a first-order Taylor series about the nominal location of the critical points and then set to zero to obtain the location of actual critical points.

Towards this end, consider an expansion point R in the neighborhood of the critical point $\hat{R}$. Approximating $dF(\hat{R})/d\hat{R}$ about R and equating it to zero yield

$$\begin{aligned}\frac{dF(\hat{R})}{d\hat{R}} \approx & \sum_{k=1}^{2} -2\beta(R - R_k) f_k(R) \\ & + (\hat{R} - R) \sum_{k=1}^{2} \left(4\beta^2 (R - R_k)^2 - 2\beta\right) f_k(R) \\ & = 0.\end{aligned}$$

Thus

$$\hat{R} = R + \frac{\sum_{k=1}^{2} (R - R_k) f_k(R)}{\sum_{k=1}^{2} \left[2\beta(R - R_k)^2 - 1\right] f_k(R)}. \quad (9)$$

To obtain $\hat{R}_1$, $\hat{R}_2$, and $\hat{R}_m$, the variable R in (9) should be replaced with R_1, R_2, and $(1/2)(R_1 + R_2)$, respectively.

A. Range Resolution Measurement Definition

1) Existence of Local Minimum Requirement: As stated earlier, in order for two targets to be considered resolved, it is required that a local minimum exist between the two peaks of the pulse-compressed return. The existence of this local minimum requires that there exist a range r between R_1 and R_2 such that $dF(r)/dr = 0$ and $d^2F(r)/dr^2 > 0$, so that

$$\sum_{k=1}^{2} -2\beta(r - R_k) f_k(r) = 0 \quad (10)$$

$$\sum_{k=1}^{2} \left(4\beta^2 (r - R_k)^2 - 2\beta\right) f_k(r) > 0. \quad (11)$$

From (10) and (11), the following inequality results:

$$2\beta \left[(r - R_2)^2 - (r - R_1)(r - R_2)\right] > \frac{R_2 - R_1}{r - R_1}. \quad (12)$$

Now, assume that $R_2 > R_1$, and define the range difference as $R_d = R_2 - R_1$. Furthermore, assume without loss of generality that $R_1 = 0$. Then, (12) can be simplified as

$$2\beta r(R_d - r) > 1. \quad (13)$$

The value of r in (13) can now be replaced by $\hat{R}_m$ from (9), so that

$$\hat{R}_m = \frac{R_d}{2} + \frac{R_d}{\beta R_d^2 - 2} \frac{\sigma_1 - \sigma_2}{\sigma_1 + \sigma_2}. \quad (14)$$

Again, without loss of generality, assume that $\sigma_1 > \sigma_2$ and that

$$\sigma_2 = \alpha\sigma_1 \quad (15)$$

for some $\alpha < 1$. Then, (14) may now be written as

$$\hat{R}_m = \frac{R_d}{2} + \frac{R_d}{\beta R_d^2 - 2} \frac{1 - \alpha}{1 + \alpha}. \quad (16)$$

Substituting (16) for r in (13) yields

$$\frac{1}{2}\sqrt{\frac{(\beta R_d^2 - 2)^3}{\beta R_d^2}} > \frac{1 - \alpha}{1 + \alpha}. \quad (17)$$

Using the first-order approximation of the left-hand side of (17) with respect to the quantity βR_d^2 results in the following inequality:

$$\beta R_d^2 > \psi_{\mathrm{LM}}(\alpha) \quad (18)$$

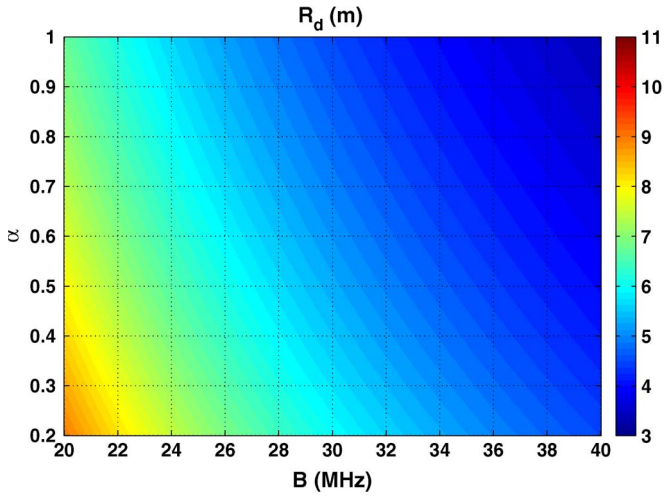

Fig. 2. Contour of range resolution using (20) as a function of ratio of target strength and waveform bandwidth.

where

$$\psi_{\mathrm{LM}}(\alpha) = \frac{3\sqrt{3}}{2}\left(\frac{\sqrt{3}}{2} + \frac{1-\alpha}{1+\alpha}\right) \tag{19}$$

and the subscript "LM" denotes "local minimum." By substituting (2) into (18), the following expression results:

$$R_d > \frac{c}{4B}\sqrt{\frac{\psi_{\mathrm{LM}}(\alpha)}{\ln 2}}. \tag{20}$$

The expression in (20) *represents a measurement definition of range resolution that accounts for both waveform bandwidth and the difference in target strength*. It is observed that when $\alpha = 1$ (equal strength targets), (20) becomes $R_d > c/2.2B$, whereas for a small value of α such as $\alpha = 0.2$, (20) becomes $R_d > c/1.7B$, indicating that the size of a resolution cell increases by 30% when the strength of the targets differ by 14 dB. Note that due to the use of approximations and the assumption of the presence of two targets, (20) is not valid for values of α approaching zero.

Fig. 2 shows a contour plot of (20), where the contour represents the range resolution as a function of the ratio of the strength of the targets $\sigma_2/\sigma_1 = \alpha$ and the waveform bandwidth.

2) Maximum Target Location Deviation Requirement: The development thus far has considered only conditions under which a local minimum exists between $\hat{R}_1$ and $\hat{R}_2$. In this section, the measurement definition for range resolution will be extended to conditions that limit the deviation of $\hat{R}_1$ and $\hat{R}_2$ from their true respective values of R_1 and R_2.

From (9), it is observed that

$$\hat{R}_k = R_k + \rho_k \tag{21}$$

for $k = 1, 2$, where ρ_k represents the deviation from the true location R_k. It is desired that the magnitude of this deviation be less than some quantity Δ, i.e.,

$$|\rho_k| < \Delta. \tag{22}$$

Using (9), and assuming again that $R_1 = 0$ and $R_2 = R_d$, the following expressions may be derived:

$$|\rho_1| = \frac{\sigma_2 R_d e^{-\beta R_d^2}}{\left|\sigma_1 - \sigma_2\left(2\beta R_d^2 - 1\right)e^{-\beta R_d^2}\right|} < \Delta \tag{23}$$

$$|\rho_2| = \frac{\sigma_1 R_d e^{-\beta R_d^2}}{\left|\sigma_2 - \sigma_1\left(2\beta R_d^2 - 1\right)e^{-\beta R_d^2}\right|} < \Delta. \tag{24}$$

By using (15), the expressions in (23) and (24) may be further simplified as

$$|\rho_1| = \frac{R_d e^{-\beta R_d^2}}{\left|\frac{1}{\alpha} - \left(2\beta R_d^2 - 1\right)e^{-\beta R_d^2}\right|} < \Delta \tag{25}$$

$$|\rho_2| = \frac{R_d e^{-\beta R_d^2}}{\left|\alpha - \left(2\beta R_d^2 - 1\right)e^{-\beta R_d^2}\right|} < \Delta. \tag{26}$$

The two denominators of (25) and (26) are now examined. Observe that the maximum value of the expression $(2\beta R_d^2 - 1)e^{-\beta R_d^2}$ is $2e^{-3/2} < 1$. Since $1/\alpha > 1$, the expression between the absolute value operator in the denominator of (25) is always positive, rendering the absolute value operator unnecessary.

It may appear that the expression between the absolute value operator in the denominator of (26) can only be guaranteed positive if $\alpha > 2e^{-3/2}$, corresponding to targets differing in power by 7 dB. However, the value of βR_d^2 is constrained by (17). Using this constraint, the minimum value of βR_d^2 is two, and occurs as α approaches one. Because the expression $(2\beta R_d^2 - 1)e^{-\beta R_d^2}$ decreases monotonically for $\beta R_d^2 \geq 1.5$, the denominator of (26) can be guaranteed positive if α is selected to be larger than $(2\beta R_d^2 - 1)e^{-\beta R_d^2}$ when $\beta R_d^2 = 2$. This yields a minimum value of $\alpha = 3e^{-3}$, corresponding to targets differing in power by 16.5 dB.

By constraining the expression between the absolute value operator in the denominator of (25) and (26) to be positive, the absolute value operator may be removed. Thus

$$\rho_1 < \rho_2 < \Delta. \tag{27}$$

In order to satisfy (22), it is sufficient to impose the condition

$$\rho_2 < \Delta. \tag{28}$$

Let $\delta = \Delta/R_d$ denote the maximum allowable deviation relative to the target range separation. From (26), the condition in (28) may be expressed as

$$\alpha e^{+\beta R_d^2} - \left(2\beta R_d^2 - 1\right) > \frac{1}{\delta} \tag{29}$$

which is equivalent to the condition

$$\beta R_d^2 > \psi_{\mathrm{MD}}(\alpha, \delta) \tag{30}$$

where

$$\psi_{\mathrm{MD}}(\alpha, \delta) = \frac{1}{2}\left(1 - \frac{1}{\delta}\right) - W_{-1}\left(-\frac{\alpha}{2}e^{+\frac{1}{2}\left(1-\frac{1}{\delta}\right)}\right) \tag{31}$$

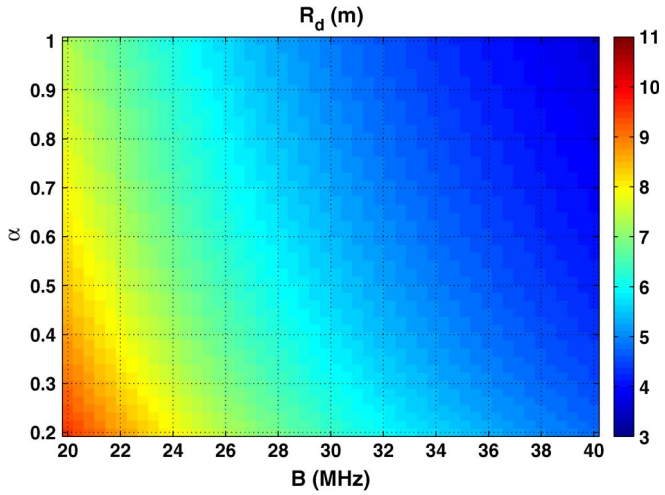

Fig. 3. Contour of range resolution using (33) as a function of ratio of target strength and waveform bandwidth for an allowable target location deviation of $\delta = 0.1$.

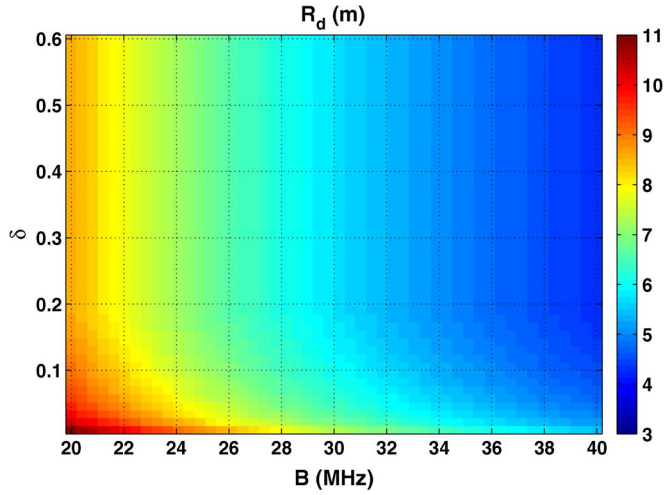

Fig. 4. Contour of range resolution using (33) as a function of allowable target location deviation and waveform bandwidth for a ratio of target strength of $\alpha = 0.3$.

and $W_n(\cdot)$ denotes the nth branch of the Lambert W function [20]. The subscript "MD" denotes "maximum deviation." By substituting (2) into (30), the following expression results:

$$R_d > \frac{c}{4B}\sqrt{\frac{\psi_{\mathrm{MD}}(\alpha,\delta)}{\ln 2}}. \tag{32}$$

The expression in (32) *represents a measurement definition of range resolution that accounts for waveform bandwidth, the difference in target strength, and the allowable deviation of the peaks in the pulse-compressed return from the true target locations*. Note that (32) cannot be used independently of (20) since larger values of δ may result in a minimum value for R_d predicted by (32) that is smaller than that allowed by (20). *Thus,* (20) *and* (32) *may be combined to yield the composite comprehensive measurement definition for range resolution*

$$R_d > \frac{c}{4B}\sqrt{\frac{\max\left(\psi_{\mathrm{LM}}(\alpha),\psi_{\mathrm{MD}}(\alpha,\delta)\right)}{\ln 2}}. \tag{33}$$

Figs. 3–5 show contour plots of (33). The contours in the three figures represent the range resolution for fixed values of the target location deviation, ratio of target strength, and waveform bandwidth, respectively. Note that in Figs. 4 and 5, the straight contour region for larger values of δ corresponds to the region in which the max operator in (33) selects $\psi_{\mathrm{LM}}(\alpha)$, whereas the curved contour region corresponds to the region in which the max operator in (33) selects $\psi_{\mathrm{MD}}(\alpha,\delta)$.

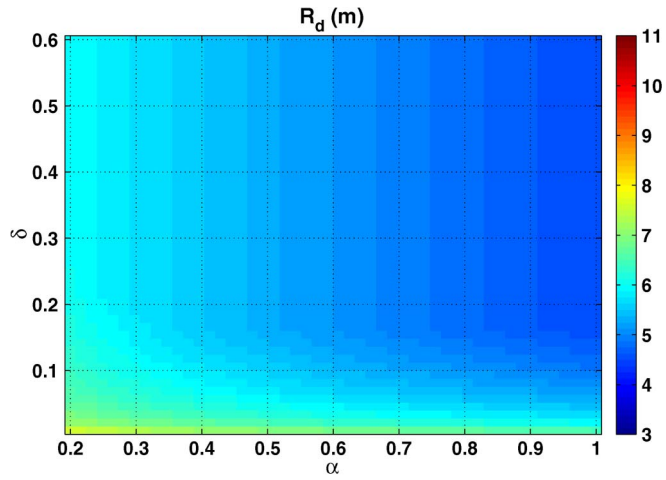

Fig. 5. Contour of range resolution using (33) as a function of allowable target location deviation and ratio of target strength for a waveform bandwidth of $B = 30$ MHz.

III. Computational and Experimental Results

Figs. 6 and 7 show contour plots of $\hat{\varepsilon}$ in (8) as a function of various parameters. Lower contour values correspond to poor resolution, while higher contour values correspond to better resolution. In these figures, contour values less than zero correspond to the white (unresolved) regions.

In Fig. 6, the contour of $\hat{\varepsilon}$ is shown as a function of the ratio of the target strength and the target range separation when the waveform bandwidth is fixed at 50 MHz. It can be seen that for a fixed range separation, resolution performance worsens as the difference in target strength increases. This is because large differences in target strength tend to result in pulse-compressed returns that resemble the ones in Fig. 1(b) and (c).

Fig. 7 shows the contour of $\hat{\varepsilon}$ as a function of the ratio of the target strength and the waveform bandwidth when the target range separation is fixed at 5 m. As in Fig. 6, it can be seen that for a fixed bandwidth in Fig. 7, the resolution performance worsens as the difference in target strength increases. Increasing range separation or waveform bandwidth (which decreases the width of the pulse-compressed waveform) improves resolution performance, since there is less interference between the pulse-compressed returns of the two targets.

The contours in Figs. 6 and 7 were plotted assuming an allowable target location deviation of $\delta = 0.1$. It can be seen in both figures that the resolution boundary computed using the measurement definition of range resolution (33) agrees well with the actual contour boundary. Figs. 6 and 7 also show the resolution boundary computed using (20). This reflects the resolution boundary when no constraint is placed on the

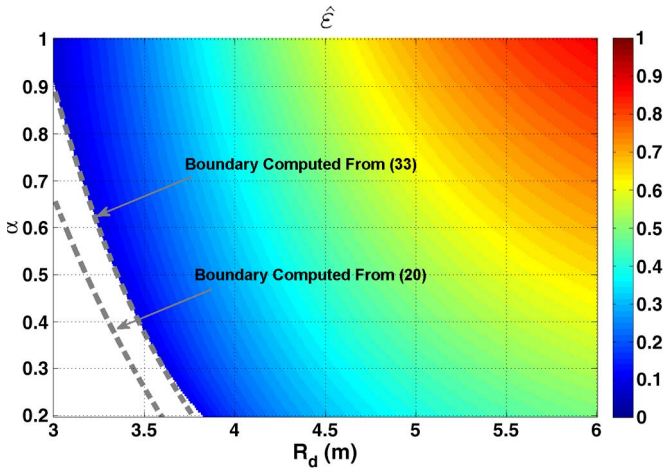

Fig. 6. Contour of (8) as a function of ratio of target strength and range separation for a waveform bandwidth of $B = 50$ MHz and an allowable target location deviation of $\delta = 0.1$.

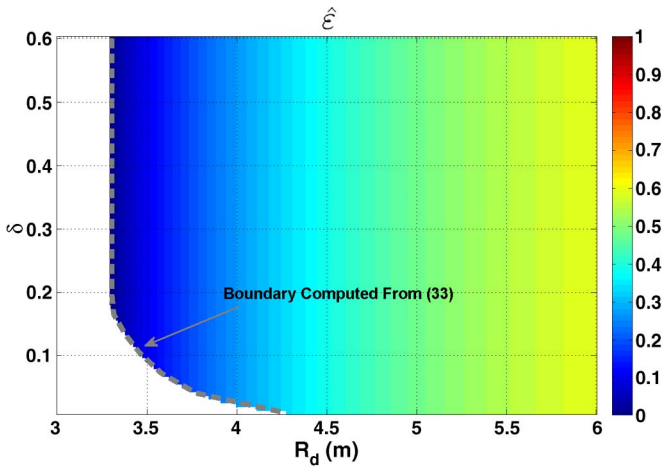

Fig. 8. Contour of (8) as a function of allowable target location deviation and range separation for a waveform bandwidth of $B = 50$ MHz and a ratio of target strength of $\alpha = 0.4$.

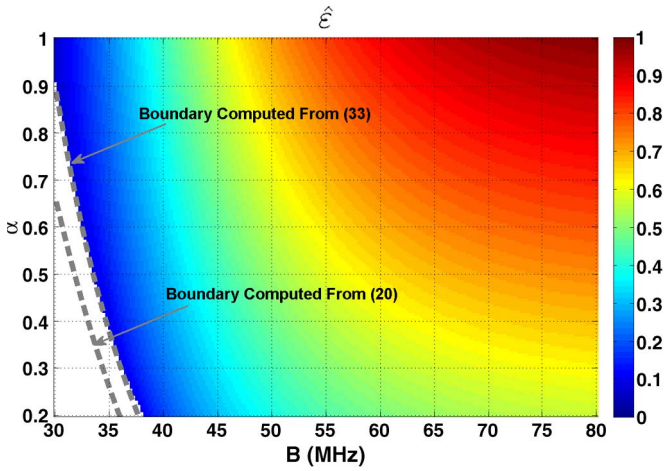

Fig. 7. Contour of (8) as a function of ratio of target strength and waveform bandwidth for a range separation of $R_d = 5$ m and an allowable target location deviation of $\delta = 0.1$.

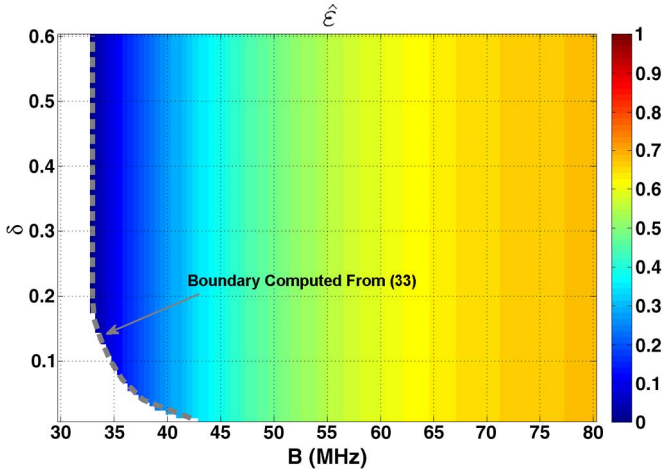

Fig. 9. Contour of (8) as a function of allowable target location deviation and waveform bandwidth for a range separation of $R_d = 5$ m and a ratio of target strength of $\alpha = 0.4$.

maximum allowable target location deviation. Hence, the resolution boundary computed from (33) is more conservative than that computed from (20).

Figs. 8 and 9 show contours of $\hat{\varepsilon}$ as a function of δ, the allowable target location deviation. It is seen in both figures that the computed resolution boundary agrees well with the actual contour boundary. The straight nature of the contours implies that the resolution quality is independent of δ. However, when the constraint placed by increasingly smaller values of δ cannot be met, resolution fails to occur. This is indicated by the curved region of the resolution boundary, which corresponds to the region in which the max operator in (33) selects $\psi_{\mathrm{MD}}(\alpha, \delta)$. The straight region of the resolution boundary corresponds to the region in which the max operator in (33) selects $\psi_{\mathrm{LM}}(\alpha)$. Note that the resolution boundary computed using (20) would be vertical (independent of δ) throughout. Thus, the area contained between the exterior of the curved region of the resolution boundary and the extension of the vertical region of the resolution boundary in Figs. 8 and 9 corresponds to the area in which resolution is lost due to the imposition of a constraint on the allowable target location deviation.

The figures in this section provide a comprehensive view of how the results in this paper may be used to determine baseline requirements when designing a system with a given desired level of range resolution performance. For example, suppose that a range resolution of 5 m is desired. A conventional calculation would assert that at least $c/(2 \times 5) = 30$ MHz of bandwidth is required. However, suppose that it is required that this resolution level be maintained for targets that differ in strength by $\alpha = 0.4$, and that the resulting target location error should not exceed $\delta = 0.1$. From Fig. 7, it can be seen that these requirements increase the minimum bandwidth to 35 MHz. Moreover, this bandwidth corresponds to the resolution boundary, where the value of $\hat{\varepsilon}$ approaches zero. As a practical matter, since a resolution algorithm must process the return signal, $\hat{\varepsilon}$ should be kept at a larger value, for example, around 0.5. This results in a final minimum required bandwidth of around 52 MHz, which, with the realistic constraints

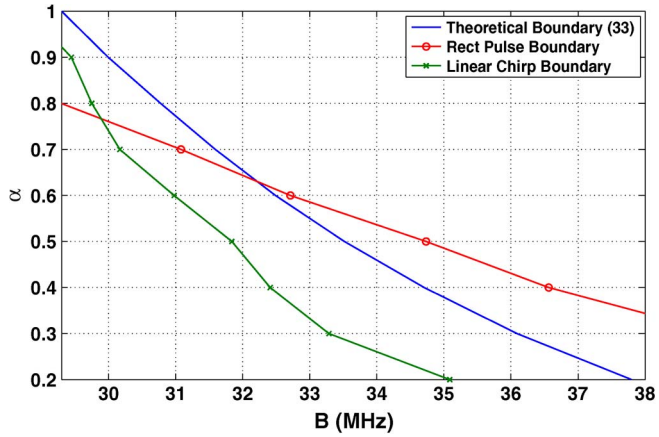

Fig. 10. Comparison of theoretical resolution boundary with actual waveforms as a function of ratio of target strength and waveform bandwidth without windowing. Range separation is fixed at $R_d = 5$ m, and an allowable target location deviation is fixed at $\delta = 0.1$.

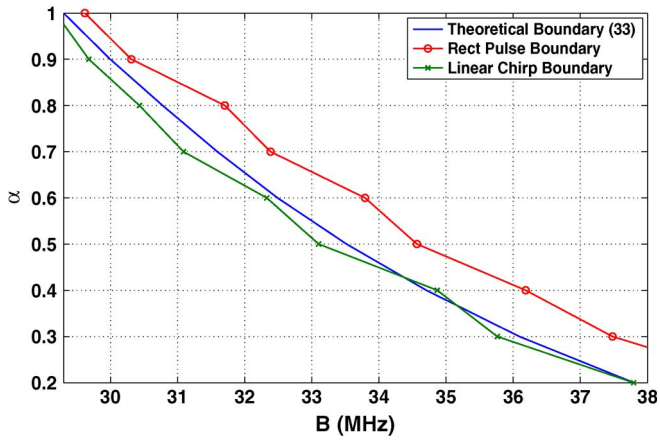

Fig. 11. Comparison of theoretical resolution boundary with actual waveforms as a function of ratio of target strength and waveform bandwidth with windowing. Range separation is fixed at $R_d = 5$ m, and an allowable target location deviation is fixed at $\delta = 0.1$.

$(\alpha, \delta, \hat{\varepsilon}) = (0.4, 0.1, 0.5)$, is nearly double the value yielded by the conventional calculation as shown earlier.

Finally, experimental verification of the derived results was carried out. In order to simulate a controlled data collection environment, an arbitrary waveform generator (AWG) was used to generate either linear chirp or rectangular pulse waveforms with a fixed range separation (delay) of $R_d = 5$ m. For each desired value of α, the resolution boundary from (33) in Fig. 7 was used to provide a starting point to estimate the required waveform bandwidth. After pulse compressing the AWG output using a digital receiver, δ and $\hat{\varepsilon}$ were computed, and the waveform bandwidth was iteratively adjusted in order to determine the actual resolution boundary. The results are shown in Fig. 10.

It can be seen from Fig. 10 that there is indeed a mismatch between the predicted theoretical resolution boundary and the actual resolution boundary for both the linear chirp and rectangular pulse waveform. This is expected, however, since the analysis presented in this paper assumed a Gaussian pulse-compressed spectrum, which, obviously, neither type of waveform satisfies. As such, for any particular waveform, the predicted boundary will never be exact but will provide a reasonable "average" approximation.

In general, the raw pulse-compressed spectrum is rarely used. In practice, windowing (tapering) is commonly applied to reduce the range sidelobes at the expense of increasing the mainlobe width. Fig. 11 shows the results of applying a Hamming window to the pulse-compressed spectrum. As expected, windowing improves the accuracy of the Gaussian shape approximation, and this improvement is especially pronounced for the linear chirp waveform.

In summary, the process described in this paper has practical implications. The analytical results provide a reasonable approximation of the resolution boundary. The methodology can be used to develop a precise resolution bound for a particular waveform to assess the impact of the relative target strength on the range resolution capability of a radar system.

IV. Conclusion

A common definition used for measuring range resolution for equal strength targets was modified for targets of unequal strength. This modification included the effects of the shifting of the critical points of the pulse-compressed return from their expected location. Conditions were developed for the existence of a local minimum between the two peaks of the pulse-compressed return, as well as limiting the deviation of these peaks from the true target locations. These conditions were used to develop a more comprehensive measurement definition of range resolution that includes the difference in target strength as well as the allowable target location deviation as specific parameters. Computational and experimental examples using the results were carried out, and these effects of various parameters were investigated to study their impact on range resolution performance.

Acknowledgment

Opinions, interpretations, conclusions, and recommendations are those of the authors and are not necessarily endorsed by the United States Government.

References

[1] A. Rihaczek, "Radar signal design for target resolution," *Proc. IEEE*, vol. 53, no. 2, pp. 116–128, Feb. 1965.
[2] L. Graham, "Synthetic interferometer radar for topographic mapping," *Proc. IEEE*, vol. 62, no. 6, pp. 763–768, Jun. 1974.
[3] D. Mensa, "Wideband radar cross section diagnostic measurements," *IEEE Trans. Instrum. Meas.*, vol. IM-33, no. 3, pp. 206–214, Sep. 1984.
[4] T. Tice, "An overview of radar cross section measurement techniques," *IEEE Trans. Instrum. Meas.*, vol. 39, no. 1, pp. 205–207, Feb. 1990.
[5] A. Jain and I. Patel, "Ground-to-air imaging radar for RCS measurements," *IEEE Trans. Instrum. Meas.*, vol. 41, no. 6, pp. 951–956, Dec. 1992.
[6] J. Odendall and J. Joubert, "Radar cross section measurements using near-field radar imaging," *IEEE Trans. Instrum. Meas.*, vol. 45, no. 6, pp. 948–954, Dec. 1996.
[7] P.-R. Wu, "A criterion for radar resolution enhancement with Burg algorithm," *IEEE Trans. Aerosp. Electron. Syst.*, vol. 31, no. 3, pp. 897–915, Jul. 1995.
[8] J. Dhanoa, E. Hughes, and R. Ormondroyd, "Simultaneous detection and parameter estimation of multiple linear chirps," in *Proc. Int. Conf. Acoust., Speech, Signal Process.*, Apr. 2003, pp. 129–132.

[9] E. Hughes, M. Lewis, and C. Alabaster, "Automatic target recognition: The problems of data separability and decision making," in *Proc. IET Semin. High Resolution Imag. Target Classification*, Nov. 2006, pp. 29–37.
[10] M. Shinriki, R. Sato, and H. Takase, "Multi-range resolution radar using sideband spectrum energy," in *Proc CIE Int. Conf. Radar*, 2006, pp. 231–235.
[11] S. Blunt, K. Gerlach, and T. Higgins, "Aspects of radar range super-resolution," in *Proc. IEEE Radar Conf.*, Apr. 2007, pp. 683–687.
[12] M. Herman and T. Strohmer, "High-resolution radar via compressed sensing," *IEEE Trans. Signal Process.*, vol. 57, no. 6, pp. 2275–2284, Jun. 2009.
[13] D. Wehner, *High-Resolution Radar*. Norwood, MA: Artech House, 1994.
[14] J. P. Skinner, B. M. Kent, R. C. Wittmann, D. L. Mensa, and D. J. Andersh, "Normalization and interpretation of radar images," *IEEE Trans. Antennas Propag.*, vol. 46, no. 4, pp. 502–506, Apr. 1998.
[15] A. Rihaczek, "Radar resolution of ideal point scatterers," *IEEE Trans. Aerosp. Electron. Syst.*, vol. 32, no. 2, pp. 842–845, Apr. 1996.
[16] H. S. Mir and J. D. Wilkinson, "Radar target resolution probability in a noise-limited environment," *IEEE Trans. Aerosp. Electron. Syst.*, vol. 44, no. 3, pp. 1234–1239, Jul. 2008.
[17] H. Mir and B. Carlson, "Resolution of unequal strength targets," in *Proc. IEEE Radar Conf.*, Sep. 2009, pp. 1–5.
[18] Q. T. Zhang, "Probability of resolution of the MUSIC algorithm," *IEEE Trans. Signal Process.*, vol. 43, no. 4, pp. 978–987, Apr. 1995.
[19] A. Ferreol, P. Larzabal, and M. Viberg, "On the resolution probability of MUSIC," *IEEE Trans. Signal Process.*, vol. 56, no. 5, pp. 1945–1953, May 2008.
[20] R. M. Corless, G. H. Gonnet, D. E. G. Hare, D. J. Jeffrey, and D. E. Knuth, "On the Lambert W function," *Adv. Comput. Math.*, vol. 5, pp. 329–359, 1996.

Hasan S. Mir (M'06–SM'10) received the B.S. (*cum laude*), M.S., and Ph.D. degrees in electrical engineering from the University of Washington, Seattle, in 2000, 2001, and 2005, respectively.

From 2005 to 2009, he was with the Air Defense Technology Group, Lincoln Laboratory, Massachusetts Institute of Technology, Lexington. Since 2009, he has been an Assistant Professor with the Department of Electrical Engineering, American University of Sharjah, Sharjah, U.A.E.

Blair D. Carlson (M'81–SM'91) received the B.S. degree in engineering science from The Pennsylvania State University, State College, in 1976 and the M.E. degree in electrical engineering from the University of Virginia, Charlottesville, in 1978.

Since 1982, he has been a member of the Technical Staff with Lincoln Laboratory, Massachusetts Institute of Technology, Lexington, involved in the areas of radar, antennas, signal processing, sonar, communications, and space situational awareness.

Mr. Carlson was the Associate Editor of the IEEE TRANSACTIONS ON ANTENNAS AND PROPAGATION for adaptive arrays from 1991 to 1994. He received the 1995 M. Barry Carlton Award from the IEEE Aerospace and Electronic Systems Society for the best paper of the year published in the Transactions.